*DOI:*
10.1016/j.jalz.2018.09.011

*Document Version*
Peer reviewed version

# A signature pattern of cortical atrophy in dementia with Lewy bodies: a study on 333 patients from The European DLB Consortium

*Oppedal K[1,2,*], Ferreira D[3,*], Cavallin L[3], Lemstra AW[4], ten Kate M[5], Padovani A[6], Rektorova I[7],Bonanni L[8], Wahlund L-O[3], Engedal K[9], Nobili F[10], Kramberger M[11], Taylor J-P[12], Hort J[13,14], Snædal J[15], Blanc F[16,17], Walker Z[18], Antonini A[19], Westman E[3,20,**] and Aarsland D[1,21,**,***] for the Alzheimer's Disease Neuroimaging Initiative#*

1. *Centre for Age-Related Medicine, Stavanger University Hospital, Stavanger, Norway*
2. *Department of Radiology, Stavanger University Hospital, Stavanger, Norway*
3. *Division of Clinical Geriatrics, Department of Neurobiology, Care Sciences and Society, Karolinska Institutet, Stockholm, Sweden*
4. *Department of Neurology and Alzheimercenter, VU Universisty Medical Center, Amsterdam, Netherlands*
5. *Department of Radiology and Alzheimercenter, VU Universisty Medical Center, Amsterdam, Netherlands*
6. *Neurology Unit, Department o Clinical and Experimental Sciences, University of Brescia, Brescia, Italy*
7. *1st Department of Neurology, Medical Faculty, St. Anne's Hospital and CEITEC, Masaryk University, Brno, Czech Republic*
8. *Department of Neuroscience Imaging and Clinical Sciences and CESI, University G d'Annunzio of Chieti-Pescara, Chieti, Italy*
9. *Norwegian Advisory Unit for Ageing and Health, Vestfold Hospital Trust and Oslo University Hospital, Oslo, Norway*
10. *Dept. of Neuroscience (DINOGMI), University of Genoa and Neurology Clinics, Polyclinic San Martino Hospital, Genoa, Italy*
11. *Department of Neurology, University Medical Centre Ljubljana, Medical faculty, University of Ljubljana, Slovenia*
12. *Newcastle University, Newcastle upon Tyne, United Kingdom*
13. *Memory Clinic, Department of Neurology, Charles University, 2nd Faculty of Medicine and Motol University Hospital, Prague, Czech Republic*
14. *International Clinical Research Center, St. Anne's University Hospital Brno, Brno, Czech Republic*
15. *Landspitali University Hospital, Reykjavik, Iceland*
16. *Memory Resource and Research Centre of Strasbourg/Colmar, CHRU de Strasbourg, Strasbourg, France*
17. *University of Strasbourg and French National Centre for Scientific Research (CNRS), ICube Laboratory and Fédération de Médecine Translationnelle de Strasbourg (FMTS), Team Imagerie Multimodale Intégrative en Santé (IMIS)/Neurocrypto, Strasbourg, France*

*18. University College London, London & Essex Partnership University NHS Foundation Trust, United Kingdom*
*19. Department of Neuroscience, University of Padua, Padua & Fondazione Ospedale San Camillo, Venezia, Venice, Italy*
*20. Department of Neuroimaging, Centre for Neuroimaging Sciences, Institute of Psychiatry, Psychology and Neuroscience, King's College London, London, UK*
*21. Institute of Psychiatry, Psychology and Neuroscience, King's College London, London, UK*

**Shared first author*
***Shared senior author*
****Corresponding author:*
Dag Aarsland
Professor and Head of Department
Department of Old Age Psychiatry
Institute of Psychiatry, Psychology & Neuroscience
King's College London
16 De Crespigny Park
London SE5 8AF
+44 (0) 20 7848 0548
daarsland@gmail.com

*# Data used in preparation of this article were obtained from the Alzheimer's Disease Neuroimaging Initiative (ADNI) database (adni.loni.usc.edu). As such, the investigators within the ADNI contributed to the design and implementation of ADNI and/or provided data but did not participate in analysis or writing of this report. A complete listing of ADNI investigators can be found at: http://adni.loni.usc.edu/wp-content/uploads/how_to_apply/ADNI_Acknowledgement_List.pd*

# Abstract

**BACKGROUND:** We explored regional brain atrophy patterns and their clinical correlates in dementia with Lewy bodies (DLB).

**METHODS:** In this multicentre study we included a total of 333 DLB patients, 352 Alzheimer's disease (AD) patients, and 233 normal controls and used medial temporal lobe atrophy (MTA), posterior atrophy (PA), and frontal atrophy (GCA-F) visual rating scales. Patients were classified according to four atrophy patterns.

**RESULTS**: DLB had higher scores on all the three atrophy scales as compared to NC, but had less MTA than AD (all p-values <0.001). A signature hippocampal-sparing pattern of regional atrophy was observed in DLB. The MRI measures showed 65% ability to discriminate between DLB and AD, and marginally contributed to the discrimination over and above the core clinical features.

**CONCLUSION**: The most common pattern of atrophy of DLB was hippocampal-sparing. Future studies should explore whether comorbid AD pathology underlies the atrophy patterns seen in DLB.

# 1 Background

Differentiating between dementia types continues to be challenging due the clinico-pathological overlap between neurodegenerative diseases [1], but is important for optimal patient care [2]. Misfolding and aggregation of the same proteins are common across different clinical phenotypes, and vice-versa, the same clinical phenotype may result from different misfolded proteins [3]. For instance, amyloid-beta (Aβ) plaques, the main pathophysiological hallmark of Alzheimer's disease (AD), are commonly found in dementia with Lewy bodies (DLB); and alpha (α)-synuclein inclusions, the key pathology in DLB, are often seen in AD brains [4]. In addition, the spatial distribution of misfolded proteins can vary within the same disease, leading to distinct disease subtypes. [5-7]. Clinical and pathological heterogeneity is also common in DLB, such as the degree of AD-type pathology [8], which influences the clinical presentation, progression, and response to treatment [9, 10]. Thus, improving differential diagnosis between neurodegenerative diseases is important in order to provide optimal patient care and better predict future needs.

Structural magnetic resonance imaging (sMRI) is a powerful means to improve differential diagnosis and unravel disease heterogeneity [11]. Patterns of brain atrophy in sMRI can reliably track the spread of neurofibrillary tangles (NFT) [7] and easily be translated to the clinical routine by assessing brain atrophy with visual rating scales [5]. These visual rating scales are quick and easy to use and are the primary method for assessing brain structural changes in a clinical setting [12, 13]. Atrophy in the medial temporal lobe, commonly measured with the medial temporal atrophy (MTA) scale [14, 15], is included in the current diagnostic criteria for AD [16, 17]. Conversely, preserved medial temporal lobe volume is listed as a supportive biomarker of DLB [18]. However, MTA does occur in DLB [19], which would detract from the usefulness of this marker in individual cases [20]. Combining the MTA scale with scales of

frontal and posterior brain atrophy may improve their diagnostic capacity [13, 21]. However, this has rarely been explored in DLB. The few sMRI studies in DLB usually include small samples (normally around 20 individuals), leading to inconsistent results. [22-24]. Thus, investigating brain atrophy in DLB in a large cohort, combining MTA with scales of frontal and posterior brain atrophy, is urgently needed in DLB.

This retrospective study capitalizes on the European DLB consortium, which includes more than 1000 DLB patients, one of the largest DLB cohorts worldwide [25]. The aims of the study were to explore 1) the regional brain atrophy pattern in DLB using clinically useful visual rating scales, 2) the ability of sMRI to discriminate between DLB and AD, and 3) the clinical correlates of MRI atrophy patterns in DLB.

# 2 Material and Methods

## 2.1 Case selection

The patients were referrals to 15 outpatient memory-, movement disorders-, geriatric medicine-, psychiatric-, and neurology clinics in Europe. We included patients with DLB, AD and normal elderly control subjects (NC) who had MRI scan available for analysis. In addition, we included scans of AD and NC from ADNI (http://adni.loni.usc.edu/, PI Michael M. Weiner) [26, 27]. The ADNI is a multi-center study from the United States and Canada that was established to develop standardized imaging techniques and biomarkers in AD research. ADNI was launched in 2003 by the National Institute on Aging, the National Institute of Biomedical Imaging and Bioengineering, the Food and Drug Administration, private pharmaceutical companies, and non-profit organizations. The number of participants and source are shown in Table C1 in Appendix C.

## 2.2 Diagnostic and clinical examination

As previously described for E-DLB [25], diagnoses were made according to the 2005 international consensus criteria for probable DLB [28], and standard diagnostic criteria for AD. Diagnosis was done by the treating physician, a group of at least two expert clinicians, or by a multidisciplinary team at a consensus diagnostic meeting based on all available clinical and diagnostic test data. Diagnostic criteria and procedures for ADNI are described in [26].

Per design, the procedures were not harmonized across centers, but a detailed history and clinical examinations including physical, neurological, and psychiatric examination, were performed by a licensed specialist. Centers were requested to record whether patients fulfilled criteria for parkinsonism, visual hallucinations, and fluctuating cognition as specified in the consensus criteria [28], based on all available information. Routine blood tests were performed. Dopamine transporter SPECT (DAT) scan was available to support the diagnosis in approximately one third of the DLB patients, and pathological confirmation in a minority. Cognitive screening was performed using the MMSE [29]. MRI was used for unstructured radiological assessment to exclude other causes for dementia but the visual rating scales were not part of the clinical diagnosis. Hence, some results in this study should be considered in the context of circularity, especially those related to MMSE and the core clinical features.

Patients with acute delirium, terminal illness, previous stroke, psychotic or bipolar disorder, craniocerebral trauma, or recently diagnosed with a major somatic illness were excluded from the current study.

## 2.3 Ethics

Local ethics committee at the individual centre approved data collection for research and the inclusion of data in this multicentre study. The patients gave their written consent to use the unidentified results of their clinical, instrumental, and laboratory investigations for research purposes.

## 2.4 MRI acquisition and visual rating scales

Various MRI scanners and protocols were used as detailed in Appendix A.

All scans were rated by an experienced radiologist (L.C.) who was blind to any clinical information including diagnosis. The rater has previously demonstrated excellent intra-rater reliability in 120 random cases: weighted κ of 0.94 and 0.89 for MTA in left and right hemispheres, respectively, 0.88 for PA, and 0.83 for GCA-F [5].

Regional atrophy was assessed with three visual rating scales based on T1-weigthed images as detailed elsewhere [21]. Briefly, atrophy in the medial temporal lobe was evaluated with the MTA scale [14]; atrophy in the posterior cortex was evaluated with the posterior atrophy (PA) scale [30]; and atrophy in the frontal lobe was evaluated with the global cortical atrophy scale – frontal subscale (GCA-F) [31]. The MTA scale scores the degree of atrophy from zero to four in the hippocampus, parahippocampal gyrus, entorhinal cortex, and the surrounding cerebrospinal fluid spaces. The PA scale scores the degree of atrophy from zero to three in the posterior cingulate sulcus, precuneus, parieto-occipital sulcus and the parietal cortex. The GCA-F scale scores the degree of atrophy from zero to three in the frontal lobe as delimited by the central sulcus, the frontal bone, and the fissure of Sylvius. In the three visual rating scales, a score of zero denotes no atrophy, whereas scores from one to three/four indicate an increasing

degree of atrophy. MTA analysis was based on coronal reconstructions, GCA-F on axial reconstructions, and PA on reconstructions from all three planes.

Patterns of atrophy were investigated by combining the scores from MTA, GCA-F, and PA. Each case was classified according to our previously described system [5] giving four distinct atrophy patterns: Typical AD, limbic-predominant AD, hippocampal-sparing AD, and minimal-atrophy AD. Typical AD was defined as abnormal MTA together with abnormal PA and/or abnormal GCA-F. Limbic-predominant was defined as abnormal MTA alone with normal PA and GCA-F. Hippocampal-sparing included abnormal PA and/or abnormal GCA-F, but normal MTA. Minimal atrophy AD was defined as normal scores in MTA, PA, and GCA-F. Deviation from normality was established following previously published cut-offs [21]. The MTA scores ≥1.5, ≥1.5, ≥2, ≥2.5 were considered abnormal for the respective age ranges 45–64, 65–74, 75–84, and 85–94 years. Since an age-correction does not improve PA and GCA-F diagnostic performance, a score ≥1 was considered abnormal irrespectively of the age range [21]. More information regarding these subtypes can be found elsewhere [5]. Figure D.1 in Appendix D shows visual examples of characteristic cases.

## 2.5 Statistics

The main interest in this study was the potential differences between DLB and NC, as well as between DLB and AD. Thus, pair-wise models were conducted as described below and in Appendix B, including all the variables of interest to investigate their effect simultaneously and reducing the number of comparisons [32]. A third pair-wise model for the comparison between AD and NC is also reported for completeness of information. All the p-values reported are two-sided and were considered significant when ≤0.05. Further, p-values were adjusted with the Hochberg's correction for multiple testing as stated in the results section [33]

The demographic and clinical data were pair-wise compared across the study groups using logistic regression. Diagnosis was included as the Y variable and age, sex, education, and MMSE, as the predictors. The associations of these variables with the visual rating scales and with themselves in the DLB patients are shown in Figure 1. Further details on these analyses are provided in the Appendix B. Based on this, we included age and sex as the main confounding variables in all the models. Sensitivity analyses were also conducted by including education as extra confounding variable (as well as MMSE when comparing the AD and DLB groups).

The GCA-F and PA scales were pair-wise compared across the study groups by using ordinal regression because of their ordinal nature. The GCA-F and PA ratings were included as Y variables, and diagnosis, age, sex, education, and MMSE as predictors in two separate models. A similar model using multiple linear regression was conducted for MTA (average of left and right). Mixed ANCOVA was used to analyze the interaction between a between-subjects factor (diagnosis, 3 levels) and a within-subjects factor (visual rating scale, 3 levels). Age, sex, education, and MMSE were included as covariate variables. MTA scores were converted to a scale of 0 to 3 in the Mixed ANCOVA to allow comparison with the GCA-F and PA scores. Conversion consisted of multiplying MTA scores by a factor of 0.75 [21].

The frequency of each atrophy subtype was compared across the three groups using one-way ANOVA. The frequency of the different subtypes was compared within each diagnostic group against a random distribution using the Chi square test. The details of stepwise analyses performed to investigate how well the visual ratings discriminate between DLB and AD

patients, as well as to investigate the association between the visual ratings and the core clinical features in the DLB patients are described in Appendix B.

# 3 Results

## 3.1 Cohort characteristics

There were demographic and clinical differences between the groups (Table 1). The associations of these variables with the visual rating scales and with themselves in the DLB patients are shown in Figure 1. These differences and associations were therefore adjusted for in the analyses. The scores of the three visual rating scales are presented in Table 2. The mixed ANCOVA showed a significant interaction between study group (DLB *vs.* AD *vs.* NC) and visual rating scale (MTA *vs.* GCA-F *vs.* PA) ($F_{(4, 1583)}$=20.148; p<0.001) (age and sex included as covariate variables) (Figure 2a). The DLB group had significantly more atrophy on all rating scales compared to the NC (all p-values <0.001). Compared to AD, DLB had less MTA (p<0.001), but the groups did not differ significantly in GCA-F and PA scores. We observed a significantly higher overall atrophy in AD (p<0.001) (Figure 2b). As described above, this effect was explained by the higher MTA score in AD. All the results reported in this paragraph remained largely the same when including education and MMSE (when comparing DLB *vs.* AD) in subsequent sensitivity analysis (data not shown).

## 3.2 Distribution of AD atrophy patterns

The distribution of the AD atrophy patterns differed between the groups, and also varied considerably within groups (Table 3). As expected most NC cases were classified in the "minimal-atrophy" group. Compared to the AD group, the DLB group included a lower proportion of "typical AD" and "limbic-predominant", but a larger proportion of "hippocampal-sparing" and "minimal-atrophy". Since hippocampal-sparing can include only posterior atrophy

(abnormal PA scores), only frontal atrophy (abnormal GCA-F scores), or both, we further explored the distribution of abnormal PA and GCA-F scores within the hippocampal-sparing pattern. The most contributing region to hippocampal-sparing was the posterior cortex, especially in the NC group. However, concurrent abnormal scores in both the PA and GCA-F scales were also frequent in DLB and AD, as compared with the NC (p=0.001 and p=0.026, respectively). Controlling for the covariates did not change this result.

### 3.3 Using visual rating scales to discriminate between DLB and AD

For all the analyses in this section, visual rating scores were dichotomized into normal (0) or abnormal (1) according to previously published cut-offs [21]. Table 4 shows the discriminative performance of several analyses conducted in a stepwise manner. MTA alone discriminated between DLB and AD with an accuracy of 64.7%. Including age, sex, and MMSE in a random forest model to control for their potential confounding effect did not modify this result substantially (accuracy = 60.7%). We then conducted another random forest model including GCA-F and PA in addition to MTA, age, sex, and MMSE. This model marginally increased the discriminative performance (accuracy = 65.8%) (Table 4).

The three visual rating scales combined with the DLB core clinical symptoms (and age, sex, and MMSE) in a new random forest model, achieved an accuracy of 90.4% to discriminate between DLB and AD, compared to 88.7% based on the core feature alone. MTA was the third variable in terms of importance, after parkinsonism and visual hallucinations, but before cognitive fluctuations (Table 4). Thus, MTA marginally improved discrimination beyond that provided by the clinical features of DLB alone. In particular, MTA made a major contribution in atypical DLB cases without parkinsonism and visual hallucinations, where a normal MTA score was able to rule in most of the DLB patients with such a profile (9 out of 11 DLB patients).

Using the atrophy patterns instead of the visual rating scales revealed comparable results and highlighted the importance of the hippocampal-sparing pattern. This means that a normal MTA score is important, but in combination with abnormal PA and/or GCA-F scores it is even more important (Table 4). Similar results were obtained when these models were repeated by including education as extra predictive variable (data not shown).

### 3.4 Association between visual rating scales and core clinical features in DLB

Among DLB patients with clinical information available (n = 275), 77.2% had parkinsonism, 58.5% had visual hallucinations, and 84.7% had cognitive fluctuations. For the following analyses, visual rating scores were dichotomized into normal (0) or abnormal (1) according to previously published cut-offs [21]. MTA was associated with a lower MMSE score (r=-0.145, p= 0.008). No significant associations were observed between GCA-F and PA and the MMSE score, nor for the three visual rating scales with any of the three DLB core clinical features (data not shown).

All analyses were repeated including only those 94 DLB patients with abnormal DAT-scan. The results were similar to those in the total group, and several of them became more pronounced (data not shown).

## 4 Discussion

Establishing the signature pattern of brain atrophy in DLB has the potential to improve diagnosis, prediction of clinical course, and treatment response. The main novelty of this multicenter study is the first-time investigation of four distinct brain atrophy patterns in DLB patients, and its comparison with the distribution seen in AD. As a consequence, we have identified the signature atrophy pattern of DLB in the largest cohort reported to date. Although

we found widespread atrophy across medial temporal, frontal, and parietal lobes as compared to controls, DLB patients had less overall atrophy than the AD patients. In particular, DLB had less MTA than AD, but still showed PA and GCA-F atrophy, which indicates a higher frequency of the hippocampal-sparing pattern as compared to AD. Thus, the signature pattern of brain atrophy in DLB is hippocampal-sparing. Further, we also observed that MRI marginally improves the discrimination between DLB and AD over and above that of the core clinical features alone. In particular, MRI had greatest importance when discriminating atypical DLB cases without parkinsonism and visual hallucinations.

Relative preservation of medial temporal lobe is listed as a "supportive biomarker" in the recently revised diagnostic criteria for DLB [18]. MTA alone could discriminate between DLB and AD with 64.7% accuracy, and contributed to the classification together with the core clinical features. However, a novel contribution of our study to the revised diagnostic criteria for DLB is that, indeed, lack of MTA is important, but more important is lack of MTA with the presence of atrophy in the posterior cortex (and/or the frontal cortex). This is by definition the hippocampal-sparing pattern. Thus, we suggest that relative preservation of medial temporal lobes concurrent with a marked PA and/or GCA-F supports the diagnosis of DLB, especially in cases showing inconsistent or absent core clinical features. The clinical utility of this finding should be explored in future studies and perhaps encourage a refinement of the MRI criteria in the current diagnostic criteria for DLB [18]. In particular, the clinical discrimination between DLB and AD patients with a hippocampal-sparing pattern needs to be further explored.

The emergence of the hippocampal-sparing pattern in our study also aligns with another relevant functional biomarker of DLB, i.e. the cingulate island sign and occipital hypoperfusion on $^{18}$F-fluorodeoxyglucose positron emission tomography (FDG-PET). The cingulate island

sign reflects sparing of the posterior cingulate cortex relative to the precuneus and cuneus [34]. Combining MRI and FDG-PET findings could potentially increase the accuracy of DLB diagnosis.

There is a remarkable pathological heterogeneity in DLB. Most DLB patients have some degree of AD pathology, which varies from sparse to severe [8]. MTA is associated with degree of tau pathology [35], thus more MTA can be seen as a proxy of AD [34]. This interpretation aligns with the data from Whitwell et al. [7], where 42% of the AD patients with a hippocampal-sparing pattern had DLB pathology, while only 30% of those with a typical AD or a limbic-predominant pattern had DLB pathology. Based on CSF analyses, AD pathology in DLB is associated with a more AD-like clinical phenotype [10], more rapid progression of dementia [36], and less response to cholinesterase inhibitors [9]. Thus, in addition to aiding in the differential diagnosis, the MRI atrophy pattern may provide information regarding the future rate of decline, which has been demonstrated in AD patients [5]. However, there are at present only few longitudinal DLB studies, with small samples. Thus, investigating AD pathology in DLB patterns of atrophy is warranted.

We observed less overall structural atrophy in DLB compared to AD, with similar dementia severity. This suggests that functional brain changes, which are potentially reversible and amenable to drug therapy, may be more important in DLB compared to AD. For example, relatively more and earlier cholinergic deficits have been reported in DLB compared to AD [37], which could lead to better response to cholinergic agents [38].

Relatively little is known about the underlying mechanisms of the core clinical features in DLB. We found no significant associations between regional atrophy and the core DLB features.

Previous studies conducted in smaller samples suggested that motor symptoms are associated with nigrostriatal pathology [39, 40]. A recent longitudinal study found that progression of parkinsonism was associated with greater whole brain atrophy as well as more hippocampus and amygdala atrophy [35]. In our study, MTA was significantly associated with cognitive impairment (i.e. lower MMSE score), consistent with previous studies [34]. Visual hallucinations have been found to be related to occipital pathology [41], but we did not observe any significant association between visual hallucinations and scores in the PA scale. However, although one of the criteria of the PA scale is widening of the parieto-occipital sulcus [30], and higher scores in the PA scale correlate with less gray matter in the occipital cortex [42], the PA scale was not designed to measure atrophy specifically in the occipital lobe. More detailed analyses including automated methods for image data processing and analysis, for example voxel-based morphometry or cortical thickness studies, may be needed to explore the structural brain-correlates of these clinical features.

To our knowledge, this is the largest DLB cohort with MRI scans reported to date. The main limitation is the retrospective design, and thus, the diagnostic, clinical, and imaging procedures were not harmonized. To overcome the imaging issue, we applied visual rating scales of brain atrophy, performed by one rater across all centers, which are robust to variability in scanning parameters. Differences in age, sex, education, and MMSE scores were adjusted for throughout the statistical analyses. Diagnoses were mainly clinical, with only a subgroup having dopamine transporter SPECT and a minority with autopsy studies. Thus, some degree of misdiagnosis cannot be excluded, for example, with some DLB patients being diagnosed as AD and vice versa. However, these limitations often lead to increased noise, thus reducing the possibility to identify small effect sizes and associations. Consistent with this, findings were similar or even more pronounced in the DLB subgroup with abnormal DAT scan. Hence, the observed findings

in this large cohort are likely robust. However, to improve diagnostic accuracy, future studies should aim at including diagnostic markers highly specific for DLB, such as DAT scan, metaiodobenzylguanidine scan, and polysomnography [18], and aim towards including a substantial subgroup of patients with autopsy-confirmed diagnosis. Visual rating scales are less sensitive than automated methods for image processing and analysis, and are subject to rater bias. For this reason, all the scans were rated by a single experienced rater who has previously demonstrated high reliability [5]. Furthermore, numerous previous studies have validated MTA, PA, and GCA-F against automated imaging methods [31, 42-44], including pathologically diagnosed dementia cases [45]. Visual rating scales are simple and quick [12, 13, 21] and, thus, much more likely to be used in clinical practice, strengthening the real-world impact of our findings. Nonetheless, reliable ratings rely on experienced raters, which could limit the generalizability of this procedure to centers with less experienced raters. Finally, circularity cannot be excluded for MMSE and the core clinical features in this study. MRI was visually assessed in an unstructured manner as part of the diagnostic procedure, but is not a core feature of DLB and thus was not used for the diagnosis of DLB in this cohort. Since our focus was brain atrophy, this issue highlights the discriminative value of MRI when compared to the core clinical criteria. With the inclusion of biomarkers as part of the diagnostic criteria for both DLB and AD, there will always be a risk for circularity, as previously discussed [12, 51].

In conclusion, we have shown that DLB patients have widespread cortical atrophy, but compared to AD, DLB patients have less overall atrophy following a signature pattern consisting of a hippocampal-sparing type. Future studies should explore AD pathological comorbidity underlying these atrophy patterns in DLB, apply more detailed measurements of cortical and subcortical structures in large DLB cohorts, and explore their ability to predict key clinical features.

# 5 References


[1] Rivero-Santana A, Ferreira D, Perestelo-Perez L, Westman E, Wahlund LO, Sarria A, et al. Cerebrospinal Fluid Biomarkers for the Differential Diagnosis between Alzheimer's Disease and Frontotemporal Lobar Degeneration: Systematic Review, HSROC Analysis, and Confounding Factors. J Alzheimers Dis. 2017;55:625-44.

[2] Winblad B, Amouyel P, Andrieu S, Ballard C, Brayne C, Brodaty H, et al. Defeating Alzheimer's disease and other dementias: a priority for European science and society. Lancet Neurol. 2016;15:455-532.

[3] Villemagne VL, Fodero-Tavoletti MT, Masters CL, Rowe CC. Tau imaging: early progress and future directions. Lancet Neurol. 2015;14:114-24.

[4] Toledo JB, Cairns NJ, Da X, Chen K, Carter D, Fleisher A, et al. Clinical and multimodal biomarker correlates of ADNI neuropathological findings. Acta Neuropathol Commun. 2013;1:65.

[5] Ferreira D, Verhagen C, Hernandez-Cabrera JA, Cavallin L, Guo CJ, Ekman U, et al. Distinct subtypes of Alzheimer's disease based on patterns of brain atrophy: longitudinal trajectories and clinical applications. Sci Rep. 2017;7:46263.

[6] Murray ME, Graff-Radford NR, Ross OA, Petersen RC, Duara R, Dickson DW. Neuropathologically defined subtypes of Alzheimer's disease with distinct clinical characteristics: a retrospective study. Lancet Neurol. 2011;10:785-96.

[7] Whitwell JL, Dickson DW, Murray ME, Weigand SD, Tosakulwong N, Senjem ML, et al. Neuroimaging correlates of pathologically defined subtypes of Alzheimer's disease: a case-control study. Lancet Neurol. 2012;11:868-77.

[8] Howlett DR, Whitfield D, Johnson M, Attems J, O'Brien JT, Aarsland D, et al. Regional Multiple Pathology Scores Are Associated with Cognitive Decline in Lewy Body Dementias. Brain Pathol. 2015;25:401-8.

[9] Graff-Radford J, Boeve BF, Pedraza O, Ferman TJ, Przybelski S, Lesnick TG, et al. Imaging and acetylcholinesterase inhibitor response in dementia with Lewy bodies. Brain. 2012;135:2470-7.

[10] Lemstra AW, de Beer MH, Teunissen CE, Schreuder C, Scheltens P, van der Flier WM, et al. Concomitant AD pathology affects clinical manifestation and survival in dementia with Lewy bodies. J Neurol Neurosurg Psychiatry. 2017;88:113-8.

[11] Poulakis K, Pereira JB, Mecocci P, Vellas B, Tsolaki M, Kłoszewska I, et al. Heterogeneous patterns of brain atrophy in Alzheimer's disease. Neurobiology of Aging. 2018.

[12] Ferreira D, Jelic V, Cavallin L, Oeksengaard AR, Snaedal J, Hogh P, et al. Electroencephalography Is a Good Complement to Currently Established Dementia Biomarkers. Dement Geriatr Cogn Disord. 2016;42:80-92.

[13] Harper L, Fumagalli GG, Barkhof F, Scheltens P, O'Brien JT, Bouwman F, et al. MRI visual rating scales in the diagnosis of dementia: evaluation in 184 post-mortem confirmed cases. Brain. 2016;139:1211-25.

[14] Scheltens P, Leys D, Barkhof F, Huglo D, Weinstein HC, Vermersch P, et al. Atrophy of medial temporal lobes on MRI in "probable" Alzheimer's disease and normal ageing: diagnostic value and neuropsychological correlates. J Neurol Neurosurg Psychiatry. 1992;55:967-72.

[15] Pereira JB, Cavallin L, Spulber G, Aguilar C, Mecocci P, Vellas B, et al. Influence of age, disease onset and ApoE4 on visual medial temporal lobe atrophy cut-offs. J Intern Med. 2014;275:317-30.

[16] Dubois B, Feldman HH, Jacova C, Hampel H, Molinuevo JL, Blennow K, et al. Advancing research diagnostic criteria for Alzheimer's disease: the IWG-2 criteria. Lancet Neurol. 2014;13:614-29.
[17] McKhann GM, Knopman DS, Chertkow H, Hyman BT, Jack CR, Jr., Kawas CH, et al. The diagnosis of dementia due to Alzheimer's disease: recommendations from the National Institute on Aging-Alzheimer's Association workgroups on diagnostic guidelines for Alzheimer's disease. Alzheimers Dement. 2011;7:263-9.
[18] McKeith IG, Boeve BF, Dickson DW, Halliday G, Taylor JP, Weintraub D, et al. Diagnosis and management of dementia with Lewy bodies: Fourth consensus report of the DLB Consortium. Neurology. 2017;89:88-100.
[19] Barkhof F, Polvikoski TM, van Straaten EC, Kalaria RN, Sulkava R, Aronen HJ, et al. The significance of medial temporal lobe atrophy: a postmortem MRI study in the very old. Neurology. 2007;69:1521-7.
[20] Barber R, Ballard C, McKeith IG, Gholkar A, O'Brien JT. MRI volumetric study of dementia with Lewy bodies: a comparison with AD and vascular dementia. Neurology. 2000;54:1304-9.
[21] Ferreira D, Cavallin L, Larsson EM, Muehlboeck JS, Mecocci P, Vellas B, et al. Practical cut-offs for visual rating scales of medial temporal, frontal and posterior atrophy in Alzheimer's disease and mild cognitive impairment. J Intern Med. 2015;278:277-90.
[22] Beyer MK, Larsen JP, Aarsland D. Gray matter atrophy in Parkinson disease with dementia and dementia with Lewy bodies. Neurology. 2007;69:747-54.
[23] Watson R, O'Brien JT, Barber R, Blamire AM. Patterns of gray matter atrophy in dementia with Lewy bodies: a voxel-based morphometry study. Int Psychogeriatr. 2012;24:532-40.
[24] Whitwell JL, Weigand SD, Shiung MM, Boeve BF, Ferman TJ, Smith GE, et al. Focal atrophy in dementia with Lewy bodies on MRI: a distinct pattern from Alzheimer's disease. Brain. 2007;130:708-19.
[25] Kramberger MG, Auestad B, Garcia-Ptacek S, Abdelnour C, Olmo JG, Walker Z, et al. Long-Term Cognitive Decline in Dementia with Lewy Bodies in a Large Multicenter, International Cohort. J Alzheimers Dis. 2017;57:787-95.
[26] Jack CR, Jr., Bernstein MA, Fox NC, Thompson P, Alexander G, Harvey D, et al. The Alzheimer's Disease Neuroimaging Initiative (ADNI): MRI methods. J Magn Reson Imaging. 2008;27:685-91.
[27] Westman E, Simmons A, Muehlboeck JS, Mecocci P, Vellas B, Tsolaki M, et al. AddNeuroMed and ADNI: similar patterns of Alzheimer's atrophy and automated MRI classification accuracy in Europe and North America. Neuroimage. 2011;58:818-28.
[28] McKeith IG, Dickson DW, Lowe J, Emre M, O'Brien JT, Feldman H, et al. Diagnosis and management of dementia with Lewy bodies: third report of the DLB Consortium. Neurology. 2005;65:1863-72.
[29] Folstein MF, Folstein SE, McHugh PR. "Mini-mental state". A practical method for grading the cognitive state of patients for the clinician. J Psychiatr Res. 1975;12:189-98.
[30] Koedam EL, Lehmann M, van der Flier WM, Scheltens P, Pijnenburg YA, Fox N, et al. Visual assessment of posterior atrophy development of a MRI rating scale. Eur Radiol. 2011;21:2618-25.
[31] Ferreira D, Cavallin L, Granberg T, Lindberg O, Aguilar C, Mecocci P, et al. Quantitative validation of a visual rating scale for frontal atrophy: associations with clinical status, APOE e4, CSF biomarkers and cognition. Eur Radiol. 2016;26:2597-610.

[32] Ferreira D, Hansson O, Barroso J, Molina Y, Machado A, Hernandez-Cabrera JA, et al. The interactive effect of demographic and clinical factors on hippocampal volume: A multicohort study on 1958 cognitively normal individuals. Hippocampus. 2017;27:653-67.
[33] Hochberg Y, Benjamini Y. More powerful procedures for multiple significance testing. Stat Med. 1990;9:811-8.
[34] Elder GJ, Mactier K, Colloby SJ, Watson R, Blamire AM, O'Brien JT, et al. The influence of hippocampal atrophy on the cognitive phenotype of dementia with Lewy bodies. Int J Geriatr Psychiatry. 2017;32:1182-9.
[35] Nedelska Z, Ferman TJ, Boeve BF, Przybelski SA, Lesnick TG, Murray ME, et al. Pattern of brain atrophy rates in autopsy-confirmed dementia with Lewy bodies. Neurobiol Aging. 2015;36:452-61.
[36] Abdelnour C, van Steenoven I, Londos E, Blanc F, Auestad B, Kramberger MG, et al. Alzheimer's disease cerebrospinal fluid biomarkers predict cognitive decline in lewy body dementia. Mov Disord. 2016;31:1203-8.
[37] Kotagal V, Muller ML, Kaufer DI, Koeppe RA, Bohnen NI. Thalamic cholinergic innervation is spared in Alzheimer disease compared to parkinsonian disorders. Neurosci Lett. 2012;514:169-72.
[38] Touchon J, Bergman H, Bullock R, Rapatz G, Nagel J, Lane R. Response to rivastigmine or donepezil in Alzheimer's patients with symptoms suggestive of concomitant Lewy body pathology. Curr Med Res Opin. 2006;22:49-59.
[39] Duda JE. Olfactory system pathology as a model of Lewy neurodegenerative disease. J Neurol Sci. 2010;289:49-54.
[40] Piggott MA, Perry EK, Marshall EF, McKeith IG, Johnson M, Melrose HL, et al. Nigrostriatal dopaminergic activities in dementia with Lewy bodies in relation to neuroleptic sensitivity: comparisons with Parkinson's disease. Biol Psychiatry. 1998;44:765-74.
[41] Khundakar AA, Hanson PS, Erskine D, Lax NZ, Roscamp J, Karyka E, et al. Analysis of primary visual cortex in dementia with Lewy bodies indicates GABAergic involvement associated with recurrent complex visual hallucinations. Acta Neuropathol Commun. 2016;4:66.
[42] Moller C, van der Flier WM, Versteeg A, Benedictus MR, Wattjes MP, Koedam EL, et al. Quantitative regional validation of the visual rating scale for posterior cortical atrophy. Eur Radiol. 2014;24:397-404.
[43] Bresciani L, Rossi R, Testa C, Geroldi C, Galluzzi S, Laakso MP, et al. Visual assessment of medial temporal atrophy on MR films in Alzheimer's disease: comparison with volumetry. Aging Clin Exp Res. 2005;17:8-13.
[44] Davies RR, Scahill VL, Graham A, Williams GB, Graham KS, Hodges JR. Development of an MRI rating scale for multiple brain regions: comparison with volumetrics and with voxel-based morphometry. Neuroradiology. 2009;51:491-503.
[45] Harper L, Bouwman F, Burton EJ, Barkhof F, Scheltens P, O'Brien JT, et al. Patterns of atrophy in pathologically confirmed dementias: a voxelwise analysis. J Neurol Neurosurg Psychiatry. 2017;88:908-16.

# 6 Acknowledgement, conflicts of interest and funding sources

## 6.1 Acknowledgement

Dag Aarsland is a Royal Society Wolfson Research Merit Award Holder and would like to thank the Wolfson Foundation and the Royal Society for their support.

## 6.2 Conflicts of interest

Dag Aarsland has received research support and/or honoraria from Astra-Zeneca, H. Lundbeck, Novartis Pharmaceuticals and GE Health, and served as paid consultant for H. Lundbeck, Eisai, and Evonik. The other authors have nothing to declare.

## 6.3 Funding sources

**Dag Aarsland:** "This paper represents independent research [part] funded by the National Institute for Health Research (NIHR) Biomedical Research Centre at South London and Maudsley NHS Foundation Trust and King's College London. The views expressed are those of the author(s) and not necessarily those of the NHS, the NIHR, or the Department of Health and Social Care".

**Ketil Oppedal** is funded by The Western Norway Regional Health Authority by Postdoc-grant 912152.

**Eric Westman and Daniel Ferreira** are supported by the Swedish Foundation for Strategic Research (SSF); the Strategic Research Programme in Neuroscience at Karolinska Institutet (StratNeuro); the Swedish Research Council (VR); the Åke Wiberg foundation; Hjärnfonden; Alzheimerfonden; Demensfonden; and Birgitta och Sten Westerberg.

**ADNI data:** Data collection and sharing for this project was funded by the Alzheimer's Disease Neuroimaging Initiative (ADNI) (National Institutes of Health Grant U01 AG024904) and DOD ADNI (Department of Defense award number W81XWH-12-2-0012). ADNI is funded by the National Institute on Aging, the National Institute of Biomedical

Imaging and Bioengineering, and through generous contributions from the following: AbbVie, Alzheimer's Association; Alzheimer's Drug Discovery Foundation; Araclon Biotech; BioClinica, Inc.; Biogen; Bristol-Myers Squibb Company; CereSpir, Inc.; Cogstate; Eisai Inc.; Elan Pharmaceuticals, Inc.; Eli Lilly and Company; EuroImmun; F. Hoffmann-La Roche Ltd and its affiliated company Genentech, Inc.; Fujirebio; GE Healthcare; IXICO Ltd.; Janssen Alzheimer Immunotherapy Research & Development, LLC.; Johnson & Johnson Pharmaceutical Research & Development LLC.; Lumosity; Lundbeck; Merck & Co., Inc.; Meso Scale Diagnostics, LLC.; NeuroRx Research; Neurotrack Technologies; Novartis Pharmaceuticals Corporation; Pfizer Inc.; Piramal Imaging; Servier; Takeda Pharmaceutical Company; and Transition Therapeutics. The Canadian Institutes of Health Research is providing funds to support ADNI clinical sites in Canada. Private sector contributions are facilitated by the Foundation for the National Institutes of Health (www.fnih.org). The grantee organization is the Northern California Institute for Research and Education, and the study is coordinated by the Alzheimer's Therapeutic Research Institute at the University of Southern California. ADNI data are disseminated by the Laboratory for Neuro Imaging at the University of Southern California. A complete listing of ADNI investigators can be found at: http://adni.loni.usc.edu/wp-content/uploads/how_to_apply/ADNI_Acknowledgement _List.pdf.

# 7 Keywords

dementia; Alzheimer's disease; dementia with Lewy bodies; medial temporal atrophy; posterior atrophy frontal atrophy; typical Alzheimer's disease atrophy pattern; limbic predominant atrophy pattern; hippocampal spearing atrophy pattern; minimal atrophy pattern; differential diagnosis; magnetic resonance imaging; neuroimaging

# A signature pattern of cortical atrophy in dementia with Lewy bodies: a study on 333 patients from The European DLB Consortium

*Oppedal K[1,2,*], Ferreira D[3,*], Cavallin L[3], Lemstra AW[4], ten Kate M[5], Padovani A[6], Rektorova I[7],Bonanni L[8], Wahlund L-O[3], Engedal K[9], Nobili F[10], Kramberger M[11], Taylor J-P[12], Hort J[13,14], Snædal J[15], Blanc F[16,17], Walker Z[18], Antonini A[19], Westman E[3,20,**] and Aarsland D[1,21,**,***] for the Alzheimer's Disease Neuroimaging Initiative#*

1. *Centre for Age-Related Medicine, Stavanger University Hospital, Stavanger, Norway*
2. *Department of Radiology, Stavanger University Hospital, Stavanger, Norway*
3. *Division of Clinical Geriatrics, Department of Neurobiology, Care Sciences and Society, Karolinska Institutet, Stockholm, Sweden*
4. *Department of Neurology and Alzheimercenter, VU Universisty Medical Center, Amsterdam, Netherlands*
5. *Department of Radiology and Alzheimercenter, VU Universisty Medical Center, Amsterdam, Netherlands*
6. *Neurology Unit, Department o Clinical and Experimental Sciences, University of Brescia, Brescia, Italy*
7. *1st Department of Neurology, Medical Faculty, St. Anne's Hospital and CEITEC, Masaryk University, Brno, Czech Republic*
8. *Department of Neuroscience Imaging and Clinical Sciences and CESI, University G d'Annunzio of Chieti-Pescara, Chieti, Italy*
9. *Norwegian Advisory Unit for Ageing and Health, Vestfold Hospital Trust and Oslo University Hospital, Oslo, Norway*
10. *Dept. of Neuroscience (DINOGMI), University of Genoa and Neurology Clinics, Polyclinic San Martino Hospital, Genoa, Italy*
11. *Department of Neurology, University Medical Centre Ljubljana, Medical faculty, University of Ljubljana, Slovenia*
12. *Newcastle University, Newcastle upon Tyne, United Kingdom*
13. *Memory Clinic, Department of Neurology, Charles University, 2nd Faculty of Medicine and Motol University Hospital, Prague, Czech Republic*
14. *International Clinical Research Center, St. Anne's University Hospital Brno, Brno, Czech Republic*
15. *Landspitali University Hospital, Reykjavik, Iceland*
16. *Memory Resource and Research Centre of Strasbourg/Colmar, CHRU de Strasbourg, Strasbourg, France*
17. *University of Strasbourg and French National Centre for Scientific Research (CNRS), ICube Laboratory and Fédération de Médecine Translationnelle de Strasbourg (FMTS), Team Imagerie Multimodale Intégrative en Santé (IMIS)/Neurocrypto, Strasbourg, France*

18. *University College London, London & Essex Partnership University NHS Foundation Trust, United Kingdom*
19. *Department of Neuroscience, University of Padua, Padua & Fondazione Ospedale San Camillo, Venezia, Venice, Italy*
20. *Department of Neuroimaging, Centre for Neuroimaging Sciences, Institute of Psychiatry, Psychology and Neuroscience, King's College London, London, UK*
21. *Institute of Psychiatry, Psychology and Neuroscience, King's College London, London, UK*

**Shared first author*
***Shared senior author*
****Corresponding author:*

Dag Aarsland
Professor and Head of Department
Department of Old Age Psychiatry
Institute of Psychiatry, Psychology & Neuroscience
King's College London
16 De Crespigny Park
London SE5 8AF
+44 (0) 20 7848 0548
daarsland@gmail.com

*# Data used in preparation of this article were obtained from the Alzheimer's Disease Neuroimaging Initiative (ADNI) database (adni.loni.usc.edu). As such, the investigators within the ADNI contributed to the design and implementation of ADNI and/or provided data but did not participate in analysis or writing of this report. A complete listing of ADNI investigators can be found at: http://adni.loni.usc.edu/wp-content/uploads/how_to_apply/ADNI_Acknowledgement_List.pd*

# Abstract

**BACKGROUND:** We explored regional brain atrophy patterns and their clinical correlates in dementia with Lewy bodies (DLB).

**METHODS:** In this multicentre study we included a total of 333 DLB patients, 352 Alzheimer's disease (AD) patients, and 233 normal controls and used medial temporal lobe atrophy (MTA), posterior atrophy (PA), and frontal atrophy (GCA-F) visual rating scales. Patients were classified according to four atrophy patterns.

**RESULTS**: DLB had higher scores on all the three atrophy scales as compared to NC, but had less MTA than AD (all p-values <0.001). A signature hippocampal-sparing pattern of regional atrophy was observed in DLB. The MRI measures showed 65% ability to discriminate between DLB and AD, and marginally contributed to the discrimination over and above the core clinical features.

**CONCLUSION**: The most common pattern of atrophy of DLB was hippocampal-sparing. Future studies should explore whether comorbid AD pathology underlies the atrophy patterns seen in DLB.

# 1 Background

Differentiating between dementia types continues to be challenging due the clinico-pathological overlap between neurodegenerative diseases [1], but is important for optimal patient care [2]. Misfolding and aggregation of the same proteins are common across different clinical phenotypes, and vice-versa, the same clinical phenotype may result from different misfolded proteins [3]. For instance, amyloid-beta (Aβ) plaques, the main pathophysiological hallmark of Alzheimer's disease (AD), are commonly found in dementia with Lewy bodies (DLB); and alpha (α)-synuclein inclusions, the key pathology in DLB, are often seen in AD brains [4]. In addition, the spatial distribution of misfolded proteins can vary within the same disease, leading to distinct disease subtypes. [5-7]. Clinical and pathological heterogeneity is also common in DLB, such as the degree of AD-type pathology [8], which influences the clinical presentation, progression, and response to treatment [9, 10]. Thus, improving differential diagnosis between neurodegenerative diseases is important in order to provide optimal patient care and better predict future needs.

Structural magnetic resonance imaging (sMRI) is a powerful means to improve differential diagnosis and unravel disease heterogeneity [11]. Patterns of brain atrophy in sMRI can reliably track the spread of neurofibrillary tangles (NFT) [7] and easily be translated to the clinical routine by assessing brain atrophy with visual rating scales [5]. These visual rating scales are quick and easy to use and are the primary method for assessing brain structural changes in a clinical setting [12, 13]. Atrophy in the medial temporal lobe, commonly measured with the medial temporal atrophy (MTA) scale [14, 15], is included in the current diagnostic criteria for AD [16, 17]. Conversely, preserved medial temporal lobe volume is listed as a supportive biomarker of DLB [18]. However, MTA does occur in DLB [19], which would detract from the usefulness of this marker in individual cases [20]. Combining the MTA scale with scales of

frontal and posterior brain atrophy may improve their diagnostic capacity [13, 21]. However, this has rarely been explored in DLB. The few sMRI studies in DLB usually include small samples (normally around 20 individuals), leading to inconsistent results. [22-24]. Thus, investigating brain atrophy in DLB in a large cohort, combining MTA with scales of frontal and posterior brain atrophy, is urgently needed in DLB.

This retrospective study capitalizes on the European DLB consortium, which includes more than 1000 DLB patients, one of the largest DLB cohorts worldwide [25]. The aims of the study were to explore 1) the regional brain atrophy pattern in DLB using clinically useful visual rating scales, 2) the ability of sMRI to discriminate between DLB and AD, and 3) the clinical correlates of MRI atrophy patterns in DLB.

# 2 Material and Methods

## 2.1 Case selection

The patients were referrals to 15 outpatient memory-, movement disorders-, geriatric medicine-, psychiatric-, and neurology clinics in Europe. We included patients with DLB, AD and normal elderly control subjects (NC) who had MRI scan available for analysis. In addition, we included scans of AD and NC from ADNI (http://adni.loni.usc.edu/, PI Michael M. Weiner) [26, 27]. The ADNI is a multi-center study from the United States and Canada that was established to develop standardized imaging techniques and biomarkers in AD research. ADNI was launched in 2003 by the National Institute on Aging, the National Institute of Biomedical Imaging and Bioengineering, the Food and Drug Administration, private pharmaceutical companies, and non-profit organizations. The number of participants and source are shown in Table C1 in Appendix C.

## 2.2 Diagnostic and clinical examination

As previously described for E-DLB [25], diagnoses were made according to the 2005 international consensus criteria for probable DLB [28], and standard diagnostic criteria for AD. Diagnosis was done by the treating physician, a group of at least two expert clinicians, or by a multidisciplinary team at a consensus diagnostic meeting based on all available clinical and diagnostic test data. Diagnostic criteria and procedures for ADNI are described in [26].

Per design, the procedures were not harmonized across centers, but a detailed history and clinical examinations including physical, neurological, and psychiatric examination, were performed by a licensed specialist. Centers were requested to record whether patients fulfilled criteria for parkinsonism, visual hallucinations, and fluctuating cognition as specified in the consensus criteria [28], based on all available information. Routine blood tests were performed. Dopamine transporter SPECT (DAT) scan was available to support the diagnosis in approximately one third of the DLB patients, and pathological confirmation in a minority. Cognitive screening was performed using the MMSE [29]. MRI was used for unstructured radiological assessment to exclude other causes for dementia but the visual rating scales were not part of the clinical diagnosis. Hence, some results in this study should be considered in the context of circularity, especially those related to MMSE and the core clinical features.

Patients with acute delirium, terminal illness, previous stroke, psychotic or bipolar disorder, craniocerebral trauma, or recently diagnosed with a major somatic illness were excluded from the current study.

## 2.3 Ethics

Local ethics committee at the individual centre approved data collection for research and the inclusion of data in this multicentre study. The patients gave their written consent to use the unidentified results of their clinical, instrumental, and laboratory investigations for research purposes.

## 2.4 MRI acquisition and visual rating scales

Various MRI scanners and protocols were used as detailed in Appendix A.

All scans were rated by an experienced radiologist (L.C.) who was blind to any clinical information including diagnosis. The rater has previously demonstrated excellent intra-rater reliability in 120 random cases: weighted $\kappa$ of 0.94 and 0.89 for MTA in left and right hemispheres, respectively, 0.88 for PA, and 0.83 for GCA-F [5].

Regional atrophy was assessed with three visual rating scales based on T1-weigthed images as detailed elsewhere [21]. Briefly, atrophy in the medial temporal lobe was evaluated with the MTA scale [14]; atrophy in the posterior cortex was evaluated with the posterior atrophy (PA) scale [30]; and atrophy in the frontal lobe was evaluated with the global cortical atrophy scale – frontal subscale (GCA-F) [31]. The MTA scale scores the degree of atrophy from zero to four in the hippocampus, parahippocampal gyrus, entorhinal cortex, and the surrounding cerebrospinal fluid spaces. The PA scale scores the degree of atrophy from zero to three in the posterior cingulate sulcus, precuneus, parieto-occipital sulcus and the parietal cortex. The GCA-F scale scores the degree of atrophy from zero to three in the frontal lobe as delimited by the central sulcus, the frontal bone, and the fissure of Sylvius. In the three visual rating scales, a score of zero denotes no atrophy, whereas scores from one to three/four indicate an increasing

degree of atrophy. MTA analysis was based on coronal reconstructions, GCA-F on axial reconstructions, and PA on reconstructions from all three planes.

Patterns of atrophy were investigated by combining the scores from MTA, GCA-F, and PA. Each case was classified according to our previously described system [5] giving four distinct atrophy patterns: Typical AD, limbic-predominant AD, hippocampal-sparing AD, and minimal-atrophy AD. Typical AD was defined as abnormal MTA together with abnormal PA and/or abnormal GCA-F. Limbic-predominant was defined as abnormal MTA alone with normal PA and GCA-F. Hippocampal-sparing included abnormal PA and/or abnormal GCA-F, but normal MTA. Minimal atrophy AD was defined as normal scores in MTA, PA, and GCA-F. Deviation from normality was established following previously published cut-offs [21]. The MTA scores ≥1.5, ≥1.5, ≥2, ≥2.5 were considered abnormal for the respective age ranges 45–64, 65–74, 75–84, and 85–94 years. Since an age-correction does not improve PA and GCA-F diagnostic performance, a score ≥1 was considered abnormal irrespectively of the age range [21]. More information regarding these subtypes can be found elsewhere [5]. Figure D.1 in Appendix D shows visual examples of characteristic cases.

## 2.5 Statistics

The main interest in this study was the potential differences between DLB and NC, as well as between DLB and AD. Thus, pair-wise models were conducted as described below and in Appendix B, including all the variables of interest to investigate their effect simultaneously and reducing the number of comparisons [32]. A third pair-wise model for the comparison between AD and NC is also reported for completeness of information. All the p-values reported are two-sided and were considered significant when ≤0.05. Further, p-values were adjusted with the Hochberg's correction for multiple testing as stated in the results section [33]

The demographic and clinical data were pair-wise compared across the study groups using logistic regression. Diagnosis was included as the Y variable and age, sex, education, and MMSE, as the predictors. The associations of these variables with the visual rating scales and with themselves in the DLB patients are shown in Figure 1. Further details on these analyses are provided in the Appendix B. Based on this, we included age and sex as the main confounding variables in all the models. Sensitivity analyses were also conducted by including education as extra confounding variable (as well as MMSE when comparing the AD and DLB groups).

The GCA-F and PA scales were pair-wise compared across the study groups by using ordinal regression because of their ordinal nature. The GCA-F and PA ratings were included as Y variables, and diagnosis, age, sex, education, and MMSE as predictors in two separate models. A similar model using multiple linear regression was conducted for MTA (average of left and right). Mixed ANCOVA was used to analyze the interaction between a between-subjects factor (diagnosis, 3 levels) and a within-subjects factor (visual rating scale, 3 levels). Age, sex, education, and MMSE were included as covariate variables. MTA scores were converted to a scale of 0 to 3 in the Mixed ANCOVA to allow comparison with the GCA-F and PA scores. Conversion consisted of multiplying MTA scores by a factor of 0.75 [21].

The frequency of each atrophy subtype was compared across the three groups using one-way ANOVA. The frequency of the different subtypes was compared within each diagnostic group against a random distribution using the Chi square test. The details of stepwise analyses performed to investigate how well the visual ratings discriminate between DLB and AD

patients, as well as to investigate the association between the visual ratings and the core clinical features in the DLB patients are described in Appendix B.

# 3 Results

## 3.1 Cohort characteristics

There were demographic and clinical differences between the groups (Table 1). The associations of these variables with the visual rating scales and with themselves in the DLB patients are shown in Figure 1. These differences and associations were therefore adjusted for in the analyses. The scores of the three visual rating scales are presented in Table 2. The mixed ANCOVA showed a significant interaction between study group (DLB *vs.* AD *vs.* NC) and visual rating scale (MTA *vs.* GCA-F *vs.* PA) ($F_{(4, 1583)}$=20.148; p<0.001) (age and sex included as covariate variables) (Figure 2a). The DLB group had significantly more atrophy on all rating scales compared to the NC (all p-values <0.001). Compared to AD, DLB had less MTA (p<0.001), but the groups did not differ significantly in GCA-F and PA scores. We observed a significantly higher overall atrophy in AD (p<0.001) (Figure 2b). As described above, this effect was explained by the higher MTA score in AD. All the results reported in this paragraph remained largely the same when including education and MMSE (when comparing DLB *vs.* AD) in subsequent sensitivity analysis (data not shown).

## 3.2 Distribution of AD atrophy patterns

The distribution of the AD atrophy patterns differed between the groups, and also varied considerably within groups (Table 3). As expected most NC cases were classified in the "minimal-atrophy" group. Compared to the AD group, the DLB group included a lower proportion of "typical AD" and "limbic-predominant", but a larger proportion of "hippocampal-sparing" and "minimal-atrophy". Since hippocampal-sparing can include only posterior atrophy

(abnormal PA scores), only frontal atrophy (abnormal GCA-F scores), or both, we further explored the distribution of abnormal PA and GCA-F scores within the hippocampal-sparing pattern. The most contributing region to hippocampal-sparing was the posterior cortex, especially in the NC group. However, concurrent abnormal scores in both the PA and GCA-F scales were also frequent in DLB and AD, as compared with the NC (p=0.001 and p=0.026, respectively). Controlling for the covariates did not change this result.

### 3.3 Using visual rating scales to discriminate between DLB and AD

For all the analyses in this section, visual rating scores were dichotomized into normal (0) or abnormal (1) according to previously published cut-offs [21]. Table 4 shows the discriminative performance of several analyses conducted in a stepwise manner. MTA alone discriminated between DLB and AD with an accuracy of 64.7%. Including age, sex, and MMSE in a random forest model to control for their potential confounding effect did not modify this result substantially (accuracy = 60.7%). We then conducted another random forest model including GCA-F and PA in addition to MTA, age, sex, and MMSE. This model marginally increased the discriminative performance (accuracy = 65.8%) (Table 4).

The three visual rating scales combined with the DLB core clinical symptoms (and age, sex, and MMSE) in a new random forest model, achieved an accuracy of 90.4% to discriminate between DLB and AD, compared to 88.7% based on the core feature alone. MTA was the third variable in terms of importance, after parkinsonism and visual hallucinations, but before cognitive fluctuations (Table 4). Thus, MTA marginally improved discrimination beyond that provided by the clinical features of DLB alone. In particular, MTA made a major contribution in atypical DLB cases without parkinsonism and visual hallucinations, where a normal MTA score was able to rule in most of the DLB patients with such a profile (9 out of 11 DLB patients).

Using the atrophy patterns instead of the visual rating scales revealed comparable results and highlighted the importance of the hippocampal-sparing pattern. This means that a normal MTA score is important, but in combination with abnormal PA and/or GCA-F scores it is even more important (Table 4). Similar results were obtained when these models were repeated by including education as extra predictive variable (data not shown).

### 3.4 Association between visual rating scales and core clinical features in DLB

Among DLB patients with clinical information available (n = 275), 77.2% had parkinsonism, 58.5% had visual hallucinations, and 84.7% had cognitive fluctuations. For the following analyses, visual rating scores were dichotomized into normal (0) or abnormal (1) according to previously published cut-offs [21]. MTA was associated with a lower MMSE score (r=-0.145, p= 0.008). No significant associations were observed between GCA-F and PA and the MMSE score, nor for the three visual rating scales with any of the three DLB core clinical features (data not shown).

All analyses were repeated including only those 94 DLB patients with abnormal DAT-scan. The results were similar to those in the total group, and several of them became more pronounced (data not shown).

## 4 Discussion

Establishing the signature pattern of brain atrophy in DLB has the potential to improve diagnosis, prediction of clinical course, and treatment response. The main novelty of this multicenter study is the first-time investigation of four distinct brain atrophy patterns in DLB patients, and its comparison with the distribution seen in AD. As a consequence, we have identified the signature atrophy pattern of DLB in the largest cohort reported to date. Although

we found widespread atrophy across medial temporal, frontal, and parietal lobes as compared to controls, DLB patients had less overall atrophy than the AD patients. In particular, DLB had less MTA than AD, but still showed PA and GCA-F atrophy, which indicates a higher frequency of the hippocampal-sparing pattern as compared to AD. Thus, the signature pattern of brain atrophy in DLB is hippocampal-sparing. Further, we also observed that MRI marginally improves the discrimination between DLB and AD over and above that of the core clinical features alone. In particular, MRI had greatest importance when discriminating atypical DLB cases without parkinsonism and visual hallucinations.

Relative preservation of medial temporal lobe is listed as a "supportive biomarker" in the recently revised diagnostic criteria for DLB [18]. MTA alone could discriminate between DLB and AD with 64.7% accuracy, and contributed to the classification together with the core clinical features. However, a novel contribution of our study to the revised diagnostic criteria for DLB is that, indeed, lack of MTA is important, but more important is lack of MTA with the presence of atrophy in the posterior cortex (and/or the frontal cortex). This is by definition the hippocampal-sparing pattern. Thus, we suggest that relative preservation of medial temporal lobes concurrent with a marked PA and/or GCA-F supports the diagnosis of DLB, especially in cases showing inconsistent or absent core clinical features. The clinical utility of this finding should be explored in future studies and perhaps encourage a refinement of the MRI criteria in the current diagnostic criteria for DLB [18]. In particular, the clinical discrimination between DLB and AD patients with a hippocampal-sparing pattern needs to be further explored.

The emergence of the hippocampal-sparing pattern in our study also aligns with another relevant functional biomarker of DLB, i.e. the cingulate island sign and occipital hypoperfusion on $^{18}$F-fluorodeoxyglucose positron emission tomography (FDG-PET). The cingulate island

sign reflects sparing of the posterior cingulate cortex relative to the precuneus and cuneus [34]. Combining MRI and FDG-PET findings could potentially increase the accuracy of DLB diagnosis.

There is a remarkable pathological heterogeneity in DLB. Most DLB patients have some degree of AD pathology, which varies from sparse to severe [8]. MTA is associated with degree of tau pathology [35], thus more MTA can be seen as a proxy of AD [34]. This interpretation aligns with the data from Whitwell et al. [7], where 42% of the AD patients with a hippocampal-sparing pattern had DLB pathology, while only 30% of those with a typical AD or a limbic-predominant pattern had DLB pathology. Based on CSF analyses, AD pathology in DLB is associated with a more AD-like clinical phenotype [10], more rapid progression of dementia [36], and less response to cholinesterase inhibitors [9]. Thus, in addition to aiding in the differential diagnosis, the MRI atrophy pattern may provide information regarding the future rate of decline, which has been demonstrated in AD patients [5]. However, there are at present only few longitudinal DLB studies, with small samples. Thus, investigating AD pathology in DLB patterns of atrophy is warranted.

We observed less overall structural atrophy in DLB compared to AD, with similar dementia severity. This suggests that functional brain changes, which are potentially reversible and amenable to drug therapy, may be more important in DLB compared to AD. For example, relatively more and earlier cholinergic deficits have been reported in DLB compared to AD [37], which could lead to better response to cholinergic agents [38].

Relatively little is known about the underlying mechanisms of the core clinical features in DLB. We found no significant associations between regional atrophy and the core DLB features.

Previous studies conducted in smaller samples suggested that motor symptoms are associated with nigrostriatal pathology [39, 40]. A recent longitudinal study found that progression of parkinsonism was associated with greater whole brain atrophy as well as more hippocampus and amygdala atrophy [35]. In our study, MTA was significantly associated with cognitive impairment (i.e. lower MMSE score), consistent with previous studies [34]. Visual hallucinations have been found to be related to occipital pathology [41], but we did not observe any significant association between visual hallucinations and scores in the PA scale. However, although one of the criteria of the PA scale is widening of the parieto-occipital sulcus [30], and higher scores in the PA scale correlate with less gray matter in the occipital cortex [42], the PA scale was not designed to measure atrophy specifically in the occipital lobe. More detailed analyses including automated methods for image data processing and analysis, for example voxel-based morphometry or cortical thickness studies, may be needed to explore the structural brain-correlates of these clinical features.

To our knowledge, this is the largest DLB cohort with MRI scans reported to date. The main limitation is the retrospective design, and thus, the diagnostic, clinical, and imaging procedures were not harmonized. To overcome the imaging issue, we applied visual rating scales of brain atrophy, performed by one rater across all centers, which are robust to variability in scanning parameters. Differences in age, sex, education, and MMSE scores were adjusted for throughout the statistical analyses. Diagnoses were mainly clinical, with only a subgroup having dopamine transporter SPECT and a minority with autopsy studies. Thus, some degree of misdiagnosis cannot be excluded, for example, with some DLB patients being diagnosed as AD and vice versa. However, these limitations often lead to increased noise, thus reducing the possibility to identify small effect sizes and associations. Consistent with this, findings were similar or even more pronounced in the DLB subgroup with abnormal DAT scan. Hence, the observed findings

in this large cohort are likely robust. However, to improve diagnostic accuracy, future studies should aim at including diagnostic markers highly specific for DLB, such as DAT scan, metaiodobenzylguanidine scan, and polysomnography [18], and aim towards including a substantial subgroup of patients with autopsy-confirmed diagnosis. Visual rating scales are less sensitive than automated methods for image processing and analysis, and are subject to rater bias. For this reason, all the scans were rated by a single experienced rater who has previously demonstrated high reliability [5]. Furthermore, numerous previous studies have validated MTA, PA, and GCA-F against automated imaging methods [31, 42-44], including pathologically diagnosed dementia cases [45]. Visual rating scales are simple and quick [12, 13, 21] and, thus, much more likely to be used in clinical practice, strengthening the real-world impact of our findings. Nonetheless, reliable ratings rely on experienced raters, which could limit the generalizability of this procedure to centers with less experienced raters. Finally, circularity cannot be excluded for MMSE and the core clinical features in this study. MRI was visually assessed in an unstructured manner as part of the diagnostic procedure, but is not a core feature of DLB and thus was not used for the diagnosis of DLB in this cohort. Since our focus was brain atrophy, this issue highlights the discriminative value of MRI when compared to the core clinical criteria. With the inclusion of biomarkers as part of the diagnostic criteria for both DLB and AD, there will always be a risk for circularity, as previously discussed [12, 51].

In conclusion, we have shown that DLB patients have widespread cortical atrophy, but compared to AD, DLB patients have less overall atrophy following a signature pattern consisting of a hippocampal-sparing type. Future studies should explore AD pathological comorbidity underlying these atrophy patterns in DLB, apply more detailed measurements of cortical and subcortical structures in large DLB cohorts, and explore their ability to predict key clinical features.

# 5 References

[1] Rivero-Santana A, Ferreira D, Perestelo-Perez L, Westman E, Wahlund LO, Sarria A, et al. Cerebrospinal Fluid Biomarkers for the Differential Diagnosis between Alzheimer's Disease and Frontotemporal Lobar Degeneration: Systematic Review, HSROC Analysis, and Confounding Factors. J Alzheimers Dis. 2017;55:625-44.
[2] Winblad B, Amouyel P, Andrieu S, Ballard C, Brayne C, Brodaty H, et al. Defeating Alzheimer's disease and other dementias: a priority for European science and society. Lancet Neurol. 2016;15:455-532.
[3] Villemagne VL, Fodero-Tavoletti MT, Masters CL, Rowe CC. Tau imaging: early progress and future directions. Lancet Neurol. 2015;14:114-24.
[4] Toledo JB, Cairns NJ, Da X, Chen K, Carter D, Fleisher A, et al. Clinical and multimodal biomarker correlates of ADNI neuropathological findings. Acta Neuropathol Commun. 2013;1:65.
[5] Ferreira D, Verhagen C, Hernandez-Cabrera JA, Cavallin L, Guo CJ, Ekman U, et al. Distinct subtypes of Alzheimer's disease based on patterns of brain atrophy: longitudinal trajectories and clinical applications. Sci Rep. 2017;7:46263.
[6] Murray ME, Graff-Radford NR, Ross OA, Petersen RC, Duara R, Dickson DW. Neuropathologically defined subtypes of Alzheimer's disease with distinct clinical characteristics: a retrospective study. Lancet Neurol. 2011;10:785-96.
[7] Whitwell JL, Dickson DW, Murray ME, Weigand SD, Tosakulwong N, Senjem ML, et al. Neuroimaging correlates of pathologically defined subtypes of Alzheimer's disease: a case-control study. Lancet Neurol. 2012;11:868-77.
[8] Howlett DR, Whitfield D, Johnson M, Attems J, O'Brien JT, Aarsland D, et al. Regional Multiple Pathology Scores Are Associated with Cognitive Decline in Lewy Body Dementias. Brain Pathol. 2015;25:401-8.
[9] Graff-Radford J, Boeve BF, Pedraza O, Ferman TJ, Przybelski S, Lesnick TG, et al. Imaging and acetylcholinesterase inhibitor response in dementia with Lewy bodies. Brain. 2012;135:2470-7.
[10] Lemstra AW, de Beer MH, Teunissen CE, Schreuder C, Scheltens P, van der Flier WM, et al. Concomitant AD pathology affects clinical manifestation and survival in dementia with Lewy bodies. J Neurol Neurosurg Psychiatry. 2017;88:113-8.
[11] Poulakis K, Pereira JB, Mecocci P, Vellas B, Tsolaki M, Kłoszewska I, et al. Heterogeneous patterns of brain atrophy in Alzheimer's disease. Neurobiology of Aging. 2018.
[12] Ferreira D, Jelic V, Cavallin L, Oeksengaard AR, Snaedal J, Hogh P, et al. Electroencephalography Is a Good Complement to Currently Established Dementia Biomarkers. Dement Geriatr Cogn Disord. 2016;42:80-92.
[13] Harper L, Fumagalli GG, Barkhof F, Scheltens P, O'Brien JT, Bouwman F, et al. MRI visual rating scales in the diagnosis of dementia: evaluation in 184 post-mortem confirmed cases. Brain. 2016;139:1211-25.
[14] Scheltens P, Leys D, Barkhof F, Huglo D, Weinstein HC, Vermersch P, et al. Atrophy of medial temporal lobes on MRI in "probable" Alzheimer's disease and normal ageing: diagnostic value and neuropsychological correlates. J Neurol Neurosurg Psychiatry. 1992;55:967-72.
[15] Pereira JB, Cavallin L, Spulber G, Aguilar C, Mecocci P, Vellas B, et al. Influence of age, disease onset and ApoE4 on visual medial temporal lobe atrophy cut-offs. J Intern Med. 2014;275:317-30.

[16] Dubois B, Feldman HH, Jacova C, Hampel H, Molinuevo JL, Blennow K, et al. Advancing research diagnostic criteria for Alzheimer's disease: the IWG-2 criteria. Lancet Neurol. 2014;13:614-29.
[17] McKhann GM, Knopman DS, Chertkow H, Hyman BT, Jack CR, Jr., Kawas CH, et al. The diagnosis of dementia due to Alzheimer's disease: recommendations from the National Institute on Aging-Alzheimer's Association workgroups on diagnostic guidelines for Alzheimer's disease. Alzheimers Dement. 2011;7:263-9.
[18] McKeith IG, Boeve BF, Dickson DW, Halliday G, Taylor JP, Weintraub D, et al. Diagnosis and management of dementia with Lewy bodies: Fourth consensus report of the DLB Consortium. Neurology. 2017;89:88-100.
[19] Barkhof F, Polvikoski TM, van Straaten EC, Kalaria RN, Sulkava R, Aronen HJ, et al. The significance of medial temporal lobe atrophy: a postmortem MRI study in the very old. Neurology. 2007;69:1521-7.
[20] Barber R, Ballard C, McKeith IG, Gholkar A, O'Brien JT. MRI volumetric study of dementia with Lewy bodies: a comparison with AD and vascular dementia. Neurology. 2000;54:1304-9.
[21] Ferreira D, Cavallin L, Larsson EM, Muehlboeck JS, Mecocci P, Vellas B, et al. Practical cut-offs for visual rating scales of medial temporal, frontal and posterior atrophy in Alzheimer's disease and mild cognitive impairment. J Intern Med. 2015;278:277-90.
[22] Beyer MK, Larsen JP, Aarsland D. Gray matter atrophy in Parkinson disease with dementia and dementia with Lewy bodies. Neurology. 2007;69:747-54.
[23] Watson R, O'Brien JT, Barber R, Blamire AM. Patterns of gray matter atrophy in dementia with Lewy bodies: a voxel-based morphometry study. Int Psychogeriatr. 2012;24:532-40.
[24] Whitwell JL, Weigand SD, Shiung MM, Boeve BF, Ferman TJ, Smith GE, et al. Focal atrophy in dementia with Lewy bodies on MRI: a distinct pattern from Alzheimer's disease. Brain. 2007;130:708-19.
[25] Kramberger MG, Auestad B, Garcia-Ptacek S, Abdelnour C, Olmo JG, Walker Z, et al. Long-Term Cognitive Decline in Dementia with Lewy Bodies in a Large Multicenter, International Cohort. J Alzheimers Dis. 2017;57:787-95.
[26] Jack CR, Jr., Bernstein MA, Fox NC, Thompson P, Alexander G, Harvey D, et al. The Alzheimer's Disease Neuroimaging Initiative (ADNI): MRI methods. J Magn Reson Imaging. 2008;27:685-91.
[27] Westman E, Simmons A, Muehlboeck JS, Mecocci P, Vellas B, Tsolaki M, et al. AddNeuroMed and ADNI: similar patterns of Alzheimer's atrophy and automated MRI classification accuracy in Europe and North America. Neuroimage. 2011;58:818-28.
[28] McKeith IG, Dickson DW, Lowe J, Emre M, O'Brien JT, Feldman H, et al. Diagnosis and management of dementia with Lewy bodies: third report of the DLB Consortium. Neurology. 2005;65:1863-72.
[29] Folstein MF, Folstein SE, McHugh PR. "Mini-mental state". A practical method for grading the cognitive state of patients for the clinician. J Psychiatr Res. 1975;12:189-98.
[30] Koedam EL, Lehmann M, van der Flier WM, Scheltens P, Pijnenburg YA, Fox N, et al. Visual assessment of posterior atrophy development of a MRI rating scale. Eur Radiol. 2011;21:2618-25.
[31] Ferreira D, Cavallin L, Granberg T, Lindberg O, Aguilar C, Mecocci P, et al. Quantitative validation of a visual rating scale for frontal atrophy: associations with clinical status, APOE e4, CSF biomarkers and cognition. Eur Radiol. 2016;26:2597-610.

[32] Ferreira D, Hansson O, Barroso J, Molina Y, Machado A, Hernandez-Cabrera JA, et al. The interactive effect of demographic and clinical factors on hippocampal volume: A multicohort study on 1958 cognitively normal individuals. Hippocampus. 2017;27:653-67.
[33] Hochberg Y, Benjamini Y. More powerful procedures for multiple significance testing. Stat Med. 1990;9:811-8.
[34] Elder GJ, Mactier K, Colloby SJ, Watson R, Blamire AM, O'Brien JT, et al. The influence of hippocampal atrophy on the cognitive phenotype of dementia with Lewy bodies. Int J Geriatr Psychiatry. 2017;32:1182-9.
[35] Nedelska Z, Ferman TJ, Boeve BF, Przybelski SA, Lesnick TG, Murray ME, et al. Pattern of brain atrophy rates in autopsy-confirmed dementia with Lewy bodies. Neurobiol Aging. 2015;36:452-61.
[36] Abdelnour C, van Steenoven I, Londos E, Blanc F, Auestad B, Kramberger MG, et al. Alzheimer's disease cerebrospinal fluid biomarkers predict cognitive decline in lewy body dementia. Mov Disord. 2016;31:1203-8.
[37] Kotagal V, Muller ML, Kaufer DI, Koeppe RA, Bohnen NI. Thalamic cholinergic innervation is spared in Alzheimer disease compared to parkinsonian disorders. Neurosci Lett. 2012;514:169-72.
[38] Touchon J, Bergman H, Bullock R, Rapatz G, Nagel J, Lane R. Response to rivastigmine or donepezil in Alzheimer's patients with symptoms suggestive of concomitant Lewy body pathology. Curr Med Res Opin. 2006;22:49-59.
[39] Duda JE. Olfactory system pathology as a model of Lewy neurodegenerative disease. J Neurol Sci. 2010;289:49-54.
[40] Piggott MA, Perry EK, Marshall EF, McKeith IG, Johnson M, Melrose HL, et al. Nigrostriatal dopaminergic activities in dementia with Lewy bodies in relation to neuroleptic sensitivity: comparisons with Parkinson's disease. Biol Psychiatry. 1998;44:765-74.
[41] Khundakar AA, Hanson PS, Erskine D, Lax NZ, Roscamp J, Karyka E, et al. Analysis of primary visual cortex in dementia with Lewy bodies indicates GABAergic involvement associated with recurrent complex visual hallucinations. Acta Neuropathol Commun. 2016;4:66.
[42] Moller C, van der Flier WM, Versteeg A, Benedictus MR, Wattjes MP, Koedam EL, et al. Quantitative regional validation of the visual rating scale for posterior cortical atrophy. Eur Radiol. 2014;24:397-404.
[43] Bresciani L, Rossi R, Testa C, Geroldi C, Galluzzi S, Laakso MP, et al. Visual assessment of medial temporal atrophy on MR films in Alzheimer's disease: comparison with volumetry. Aging Clin Exp Res. 2005;17:8-13.
[44] Davies RR, Scahill VL, Graham A, Williams GB, Graham KS, Hodges JR. Development of an MRI rating scale for multiple brain regions: comparison with volumetrics and with voxel-based morphometry. Neuroradiology. 2009;51:491-503.
[45] Harper L, Bouwman F, Burton EJ, Barkhof F, Scheltens P, O'Brien JT, et al. Patterns of atrophy in pathologically confirmed dementias: a voxelwise analysis. J Neurol Neurosurg Psychiatry. 2017;88:908-16.

# 6 Acknowledgement, conflicts of interest and funding sources

## 6.1 Acknowledgement

Dag Aarsland is a Royal Society Wolfson Research Merit Award Holder and would like to thank the Wolfson Foundation and the Royal Society for their support.

## 6.2 Conflicts of interest

Dag Aarsland has received research support and/or honoraria from Astra-Zeneca, H. Lundbeck, Novartis Pharmaceuticals and GE Health, and served as paid consultant for H. Lundbeck, Eisai, and Evonik. The other authors have nothing to declare.

## 6.3 Funding sources

**Dag Aarsland:** "This paper represents independent research [part] funded by the National Institute for Health Research (NIHR) Biomedical Research Centre at South London and Maudsley NHS Foundation Trust and King's College London. The views expressed are those of the author(s) and not necessarily those of the NHS, the NIHR, or the Department of Health and Social Care".

**Ketil Oppedal** is funded by The Western Norway Regional Health Authority by Postdoc-grant 912152.

**Eric Westman and Daniel Ferreira** are supported by the Swedish Foundation for Strategic Research (SSF); the Strategic Research Programme in Neuroscience at Karolinska Institutet (StratNeuro); the Swedish Research Council (VR); the Åke Wiberg foundation; Hjärnfonden; Alzheimerfonden; Demensfonden; and Birgitta och Sten Westerberg.

**ADNI data:** Data collection and sharing for this project was funded by the Alzheimer's Disease Neuroimaging Initiative (ADNI) (National Institutes of Health Grant U01 AG024904) and DOD ADNI (Department of Defense award number W81XWH-12-2-0012). ADNI is funded by the National Institute on Aging, the National Institute of Biomedical

Imaging and Bioengineering, and through generous contributions from the following: AbbVie, Alzheimer's Association; Alzheimer's Drug Discovery Foundation; Araclon Biotech; BioClinica, Inc.; Biogen; Bristol-Myers Squibb Company; CereSpir, Inc.; Cogstate; Eisai Inc.; Elan Pharmaceuticals, Inc.; Eli Lilly and Company; EuroImmun; F. Hoffmann-La Roche Ltd and its affiliated company Genentech, Inc.; Fujirebio; GE Healthcare; IXICO Ltd.; Janssen Alzheimer Immunotherapy Research & Development, LLC.; Johnson & Johnson Pharmaceutical Research & Development LLC.; Lumosity; Lundbeck; Merck & Co., Inc.; Meso Scale Diagnostics, LLC.; NeuroRx Research; Neurotrack Technologies; Novartis Pharmaceuticals Corporation; Pfizer Inc.; Piramal Imaging; Servier; Takeda Pharmaceutical Company; and Transition Therapeutics. The Canadian Institutes of Health Research is providing funds to support ADNI clinical sites in Canada. Private sector contributions are facilitated by the Foundation for the National Institutes of Health (www.fnih.org). The grantee organization is the Northern California Institute for Research and Education, and the study is coordinated by the Alzheimer's Therapeutic Research Institute at the University of Southern California. ADNI data are disseminated by the Laboratory for Neuro Imaging at the University of Southern California. A complete listing of ADNI investigators can be found at: http://adni.loni.usc.edu/wp-content/uploads/how_to_apply/ADNI_Acknowledgement _List.pdf.

# 7 Keywords

dementia; Alzheimer's disease; dementia with Lewy bodies; medial temporal atrophy; posterior atrophy frontal atrophy; typical Alzheimer's disease atrophy pattern; limbic predominant atrophy pattern; hippocampal spearing atrophy pattern; minimal atrophy pattern; differential diagnosis; magnetic resonance imaging; neuroimaging

# Response to Reviewers

We would like to thank the Editor for the opportunity to revise our manuscript. We would also like to thank the reviewers for their valuable comments. Please, find below our responses (in blue ink). Changes have also been made and tracked in the revised manuscript.

Reviewers' comments:

Reviewer #1: Although improved from the previous submission, two fundamental design flaws persist in this study. These include the 1) the issue of "circular" reasoning that has been mentioned by several previous reviewers, and 2) the lack of confirmatory diagnostic data, particularly the lack of neuropathologic autopsy finding.

We agree that these issues are relevant, and they were also addressed by Reviewer 1 and 2 for the original submission. We therefore provided a quite thorough review and comments on this for the revised version of the paper, including performing sub-analysis in the Dat scan positive cases. In addition we included an in-depth discussion of both diagnostic accuracy and the issue of circularity in the Discussion section. For this second revision, we think further discussions might not improve the paper, but suggested a sentence of how these issues can be solved in future studies.

# Research in context

1. For the literature review, commonly available medical databases were searched, as well as important review papers in the field.
2. This is the largest dementia with Lewy (DLB) cohort reported using simple and quick visual rating scales to demonstrate the characteristic the pattern of cortical atrophy characteristic of DLB. These findings can aid in the differentiation between DLB and Alzheimer's disease. However, a variety of atrophy patterns, including no atrophy, were observed in DLB.
3. Future studies should explore more detailed measurements of cortical and subcortical structures in large DLB groups, and explore whether visual atrophy patterns can predict key clinical features including rate of cognitive decline. In addition, the mechanisms underlying the cortical atrophy patterns need to be identified.

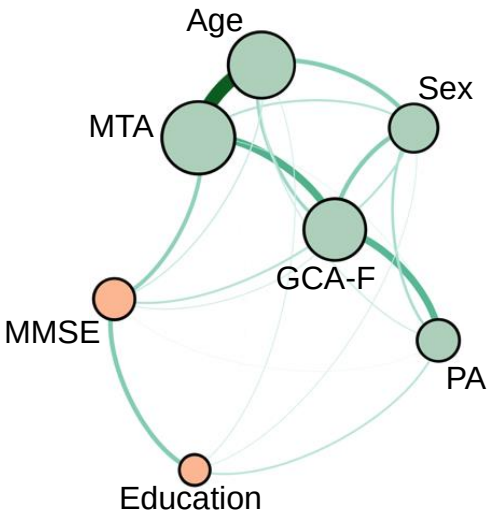


**Figure 1. Correlation between age, sex, education, MMSE, and the visual rating scales in DLB.** Weighted undirected graph with the edges showing the strength of the correlations (the thicker the edge, the higher the correlation coefficient). The size of the nodes represents the average weighted degree of each node, that is, the number of connections a node has with the rest of nodes (the larger the size, the larger number of connections). Modules are represented by colors: cluster 1 in salmon, including MMSE and education; cluster 2 in green, including age, sex, and the three visual rating scales (i.e. MTA, GCA-F and PA).

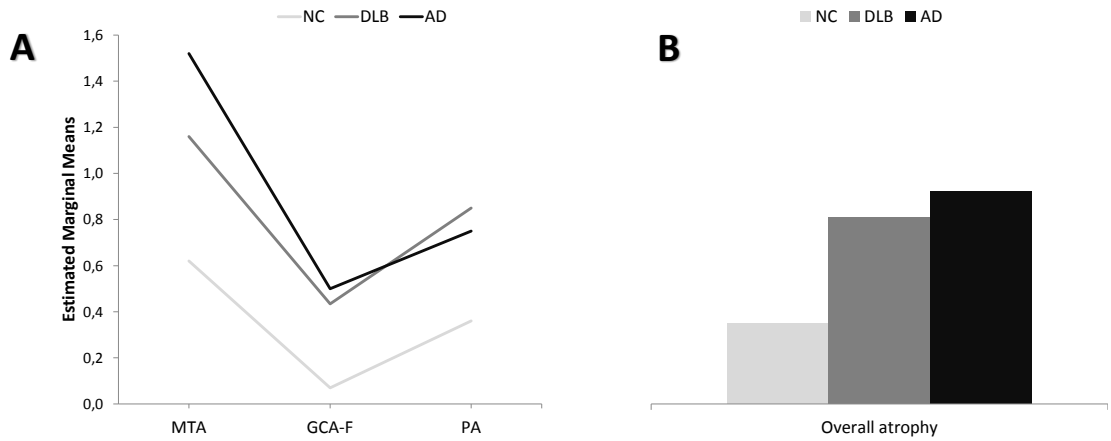


**Figure 2. Interaction between study group and visual rating scale (A), and overall degree of atrophy across groups (B).** Age and sex were included as covariate variables. Light gray, NC; Dark gray, DLB; black, AD. DLB, dementia with Lewy bodies; AD, Alzheimer's disease; NC, healthy controls; MTA, medial temporal atrophy scale; GCA-F, global frontal atrophy scale – frontal subscale; PA, posterior atrophy scale.

# TABLES

**Table 1. Patient demographics**

| | DLB (n = 333) | AD (n = 352) | NC (n = 233) | DLB *vs.* NC p-value | DLB *vs.* AD p-value | AD *vs. NC* p-value |
|---|---|---|---|---|---|---|
| Age | 73.1 (8.2) | 75.6 (7.5) | 75.5 (5.5) | **0.013** | **<0.001** | 0.411 |
| Sex, % female | 38.4 | 51.1 | 47.6 | 0.468 | **<0.001** | 0.384 |
| Education, % high | 38.4 | 63.5 | 90.5 | **<0.001** | **<0.001** | **0.004** |
| MMSE | 22.3 (4.1) | 22.9 (2.6) | 29.2 (1.0) | **<0.001** | 0.061 | **<0.001** |

Data are reported as mean(SD) for age and MMSE, and as percentage for sex and education. The variable years of education is coded as 0 (low education: less than 12 years of education) or 1 (high education: 12 years of education or more). The p-values reported in the table were obtained by conducting three separate paired logistic regression analyses for diagnosis (Y) and age, sex, education, and MMSE (predictors). The omnibus results of these three models are reported in the Appendix B. The sample size in these three models is 885 due to missing values in education. Virtually the same results are obtained in the whole sample (N = 918) when excluding education from the models (data not shown, the p-value in MMSE is 0.013 when comparing DLB and AD). DLB, dementia with Lewy bodies; AD, Alzheimer's disease; NC, healthy controls; MMSE, Mini Mental State Examination.

**Table 2. Between-group differences in visual rating scales of brain atrophy**

| | **DLB** | **AD** | **NC** | **DLB *vs.* NC** | **DLB *vs.* AD** | **AD *vs.* NC** |
|---|---|---|---|---|---|---|
| MTA, mean (SD) | 1.49 (0.86) | 2.1 (0.9) | 0.9 (0.7) | **<0.001** | **<0.001** | **<0.001** |
| Score 0, % | 6.3 | 1.7 | 24.5 | | | |
| Score 1, % | 41.7 | 21.3 | 51.5 | | | |
| Score 2, % | 34.5 | 34.7 | 21.5 | | | |
| Score 3, % | 13.2 | 31.0 | 2.6 | | | |
| Score 4, % | 4.2 | 11.4 | 0 | | | |
| GCA-F, mean (SD) | 0.41 (0.60) | 0.51 (0.65) | 0.08 (0.27) | **<0.001** | 0.157 | **<0.001** |
| Score 0, % | 64.3 | 57.7 | 91.8 | | | |
| Score 1, % | 30.0 | 33.8 | 8.2 | | | |
| Score 2, % | 5.7 | 8.5 | 0 | | | |
| Score 3, % | 0 | 0 | 0 | | | |
| PA, mean (SD) | 0.84 (0.82) | 0.76 (0.80) | 0.36 (0.64) | **<0.001** | 0.143 | **<0.001** |
| Score 0, % | 40.8 | 45.2 | 71.2 | | | |
| Score 1, % | 36.6 | 34.4 | 22.3 | | | |
| Score 2, % | 20.4 | 19.6 | 5.2 | | | |
| Score 3, % | 2.1 | 0.9 | 1.3 | | | |
| Overall atrophy, mean (SD) | 0.79 (0.16) | 0.94 (0.16) | 0.36 (0.12) | *n.a.* | **<0.001** | *n.a.* |
| 1st quartile | 6.3 | 0.9 | 88.0 | | | |
| 2nd quartile | 42.3 | 17.3 | 12.0 | | | |
| 3rd quartile | 37.2 | 31.5 | 0.0 | | | |
| 4th quartile | 14.1 | 50.3 | 0.0 | | | |

Data are reported as mean(SD) for both MTA (continuous variable) and GCA-F and PA (ordinal variables), for simplicity. The models are conducted on these data and the frequency of the scores is also reported (in percentage). The p-values reported in the table for MTA, GCA-F, and PA were obtained by conducting multiple linear regression (MTA) or ordinal regression (GCA-F and PA, separately) models with the visual rating scales as Y variables, and diagnosis, age, and sex as predictors. Education and MMSE were also included as extra predictors in the sensitivity analysis. The omnibus results of these models are reported in the Appendix B. The p-values reported in the table for overall atrophy were obtained from the mixed ANCOVA. Only the post hoc paired comparison involving DLB *vs.* AD was of interest in the current study and is thus reported. Percentages for MTA scores are based on the highest score obtained in MTA (either side) only for this table. DLB, dementia with Lewy bodies; AD, Alzheimer's disease; NC, healthy controls; n.a., non-applicable; MTA, medial temporal atrophy scale; GCA-F, global frontal atrophy scale – frontal subscale; PA, posterior atrophy scale.

**Table 3. Patterns of AD atrophy patterns in DLB, AD, and NC**

| | **DLB** | **AD** | **NC** | **DLB *vs.* NC** | **DLB *vs.* AD** | **AD *vs.* NC** |
|---|---|---|---|---|---|---|
| Typical AD | 28.8 | 50.0 | 4.3 | **<0.001** | **<0.001** | **<0.001** |
| Limbic-predominant | 9.9 | 18.2 | 7.3 | 0.350 | **0.002** | **<0.001** |
| Hippocampal-sparing | 39.3 | 19.0 | 26.2 | **0.002** | **<0.001** | 0.056 |
| Minimal-atrophy | 21.9 | 12.8 | 62.2 | **<0.001** | **0.003** | **<0.001** |
| | **<0.001** | **<0.001** | **<0.001** | | | |

Data are reported as percentage. All the p-values in this table were adjusted with the Hochberg's correction for multiple testing. DLB, dementia with Lewy bodies; AD, Alzheimer's disease; NC, healthy controls.

**Table 4. Using visual rating scales to discriminate between DLB and AD**

| Model | N | Accuracy | Sensitivity | Specificity | Variables contribution* |
|---|---|---|---|---|---|
| MTA† | 685 | 64.7 | 64.4 | 64.9 | *n.a.* |
| MTA, age, sex, MMSE | 685 | 60.7 | 57.4 | 72.4 | MTA, *Imp* = 37.6<br>MMSE, *Imp* = 21.0<br>age, *Imp* = 12.2<br>sex, *Imp* = 7.0 |
| MTA, GCA-F, PA, age, sex, MMSE | 685 | 65.8 | 55.0 | 76.1 | MTA, *Imp* = 118.2<br>MMSE, *Imp* = 61.0<br>age, *Imp* = 38.7<br>sex, *Imp* = 32.0<br>GCA-F, *Imp* = 4.2 |
| PK, VH, CF, age, sex, MMSE | 291‡ | 88.7 | 91.4 | 85.2 | PK, *Imp* = 202.2<br>VH, *Imp* = 109.0<br>CF, *Imp* = 39.5<br>MMSE, *Imp* = 21.2 |
| MTA, GCA-F, PA, PK, VH, CF, age, sex, MMSE | 291‡ | 90.4 | 91.4 | 89.1 | PK, *Imp* = 188.6<br>VH, *Imp* = 100.8<br>MTA, *Imp* = 49.1<br>CF, *Imp* = 41.2<br>MMSE, *Imp* = 21.1 |
| Atrophy patterns, age, sex, MMSE | 685 | 65.0 | 55.9 | 73.6 | MMSE, *Imp* = 18.5<br>H-S, *Imp* = 18.1<br>Typ AD, *Imp* = 17.3<br>L-P, *Imp* = 13.0<br>M-A, *Imp* = 10.6<br>age, *Imp* = 9.9<br>sex, *Imp* = 6.3 |

| | | | | | |
|---|---|---|---|---|---|
| Atrophy patterns, PK, VH, CF, age, sex, MMSE | 291‡ | 88.0 | 86.5 | 89.8 | PK, *Imp* = 236.9<br>VH, *Imp* = 115.7<br>CF, *Imp* = 63.0<br>H-S, *Imp* = 44.2<br>MMSE, *Imp* = 21.1<br>Age, *Imp* = 13.2<br>Typ AD, *Imp* = 13.2 |

*Variables that did not contributed to the model are not listed in the table;

†Sensitivity was measured as the percentage of DLB patients with a normal MTA score, and specificity as the percentage of AD patients with an abnormal MTA score.

‡Reduced N due to missing values in the DLB core clinical symptoms. n.a., non-applicable; MTA, medial temporal atrophy scale; GCA-F, global frontal atrophy scale – frontal subscale; PA, posterior atrophy scale; PK, parkinsonism; VH, visual hallucinations; CF, cognitive fluctuations; Typ AD, typical AD; H-S, hippocampal-sparing AD; L-P, limbic-predominant AD; M-A, minimal atrophy AD; Imp = importance of a given variable in the random forest, with higher values denoting greater predictive capacity.

Highlights

Overview over MRI parameters